

# Supplementary Information:

## Mechanism, kinetics and selectivity of a Williamson ether synthesis: elucidation under different reaction conditions

Aikaterini Diamanti,<sup>†,‡</sup> Zara Ganase,<sup>†</sup> Eliana Grant,<sup>†</sup> Alan Armstrong,<sup>¶</sup> Patrick  
M. Piccione,<sup>§,||</sup> Anita M. Rea,<sup>§</sup> Jeffery Richardson,<sup>⊥</sup> Amparo Galindo,<sup>†</sup> and  
Claire S. Adjiman <sup>\*,†</sup>

<sup>†</sup>*Department of Chemical Engineering, Centre for Process Systems Engineering and  
Institute for Molecular Science and Engineering, Imperial College London, South  
Kensington Campus, London SW7 2AZ, United Kingdom*

<sup>‡</sup>*Current address: Departamento de Química, Centro Universitario de Ciencias Exactas e  
Ingenierías, Universidad de Guadalajara, Jalisco, Mexico*

<sup>¶</sup>*Department of Chemistry and Institute for Molecular Science and Engineering, Imperial  
College London, Molecular Sciences Research Hub, White City Campus, Wood Lane,  
London W12 0BZ, United Kingdom*

<sup>§</sup>*Process Studies Group, Process Technology AI, Syngenta, Jealotts Hill International  
Research Center, Bracknell, Berkshire, RG42 6EY, United Kingdom*

<sup>||</sup>*Current address: F. Hoffmann-La Roche AG, Grenzacherstrasse 124, 4070 Basel,  
Switzerland.*

<sup>⊥</sup>*Discovery Research and Technologies, Eli Lilly and Company, Erl Wood Manor,  
Windlesham, Surrey, GU206PH, United Kingdom*

E-mail: c.adjiman@imperial.ac.uk

## Chemical components

Sodium  $\beta$ -naphthoxide was prepared based on the synthesis procedure described in reference (38). All other chemical reagents used in this study were purchased from Sigma-Aldrich and used without further modification. The specifications of the reagents were as follows:

- acetonitrile- $d_3$ ,  $\geq 99.8$  atom % D
- methanol- $d_4$ ,  $\geq 99.8$  atom % D, contains 0.05% (v/v) TMS
- 1,3,5-trimethoxybenzene, internal standard for quantitative NMR
- benzyl bromide, reagent grade 98%
- $\beta$ -naphthol, reagent grade 98%

## NMR peak assignment

### In acetonitrile- $d_3$

$^1\text{H}$  NMR (500MHz;  $\text{CD}_3\text{CN}$ ;  $\text{C}_6\text{H}_3(\text{OCH}_3)_3$ ):  $\delta\text{H}$

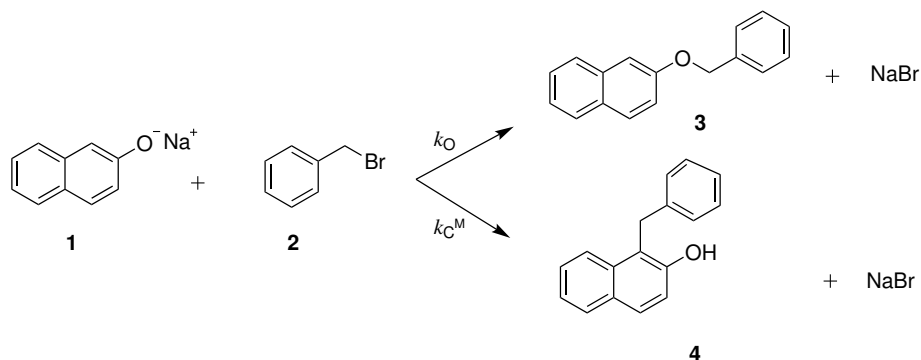
- 1,3,5-trimethoxybenzene: 3.74 (9H, s,  $(-\text{CH}_3)_3$ ), 6.10 (3H, s,  $-\text{CH}_3$ )
- sodium  $\beta$ -naphthoxide: 6.79-7.05 (1H, d,  $-\text{CH}$ )
- benzyl bromide: 4.54-4.65 (2H, s,  $-\text{CH}_2$ )
- benzyl  $\beta$ -naphthyl ether (O-alkylated product): 5.19-5.23 (2H, s,  $-\text{OCH}_2$ )
- 1-benzyl-2-naphthol (C-alkylated product): 4.36-4.47 (2H, s,  $\text{Ar}-\text{CH}_2$ )

**In methanol-d<sub>4</sub>**

<sup>1</sup>H NMR (500MHz; CD<sub>3</sub>OD; Si(CH<sub>3</sub>)<sub>4</sub>): δH

- tetramethylsilane: 0.00 (12H, s, (-CH<sub>3</sub>)<sub>4</sub>)
- sodium β-naphthoxide: 6.86-7.05 (1H, d, -CH)
- benzyl bromide: 4.51-4.55 (2H, s, CH<sub>2</sub>)
- benzyl β-naphthyl ether (O-alkylated product): 5.14-5.22 (2H, s, -OCH<sub>2</sub>)
- 1-benzyl-2-naphthol (C-alkylated product): 4.40-4.44 (2H, s, Ar-CH<sub>2</sub>)
- 1,1-dibenzyl-2-(1H)-naphthalenone (double C-alkylated product): 6.61-6.67 (4H, m, (-CH<sub>2</sub>)<sub>2</sub>)
- benzyl methyl ether: 4.41-4.44 (2H, s, -CH<sub>2</sub>)

## Minimal Model - Fittings in Acetonitrile and Methanol



Scheme S1: The reaction of sodium  $\beta$ -naphthoxide and benzyl bromide based on the Minimal model resulting to products benzyl  $\beta$ -naphthyl ether (O-alkylated product) and 1-benzyl-2-naphthol (C-alkylated product).

Table S1: Estimated reaction-rate constants  $k_O$  ( $\text{dm}^3 \text{mol}^{-1} \text{s}^{-1}$ ) and  $k_{C^M}$  ( $\text{dm}^3 \text{mol}^{-1} \text{s}^{-1}$ ) for Scheme S1 with their 95% confidence intervals (CI), obtained based on the Minimal model for acetonitrile- $\text{d}_3$  at 298 K.

Model	Parameter	Value	95% CI
Minimal model	$k_O$	$1.834 \times 10^{-2}$	$[1.154-2.513] \times 10^{-2}$
	$k_{C^M}$	$8.618 \times 10^{-4}$	$[0.000-2.311] \times 10^{-4}$

Table S2: Root-mean-square error (RMSE) (in mol dm<sup>-3</sup>) and mean absolute percentage error (MAPE) (in %) for all measurements in acetonitrile-d<sub>3</sub> at 298 K fitted with the Minimal model, and percentage rate-constant ratio (PRCR) values obtained from kinetic modelling and experiments. “Overall” refers to the average error over all data used for the model.

Model	NMR peak $j$	Species modelled	$N_j$	RMSE	MAPE	PRCR
Minimal model	6.79	<b>1</b>	8	0.0069	22.0	
	4.54	<b>2</b>	20	0.0023	9.45	
	5.19	<b>3</b>	20	0.0016	3.00	96:4
	4.36	<b>4</b>	20	0.0013	44.6	
	Overall	<b>1-4</b>	68	0.0029	19.4	
Expt.						97:3

Table S3: Estimated reaction-rate constants  $k_{\text{O}}$  (dm<sup>3</sup> mol<sup>-1</sup> s<sup>-1</sup>) and  $k_{\text{CM}}$  (dm<sup>3</sup> mol<sup>-1</sup> s<sup>-1</sup>) for Scheme S1 with their 95% confidence intervals (CI), obtained based on the Minimal model for methanol-d<sub>4</sub> at 298 K.

Model	Parameter	Value	95% CI
Minimal model	$k_{\text{O}}$	$6.856 \times 10^{-4}$	$[5.361-8.351] \times 10^{-4}$
	$k_{\text{CM}}$	$3.204 \times 10^{-4}$	$[1.811-4.597] \times 10^{-3}$

Table S4: Root-mean-square error (RMSE) (in mol dm<sup>-3</sup>) and mean absolute percentage error (MAPE) (in %) for all measurements in methanol-d<sub>4</sub> at 298 K fitted with the Minimal model, and percentage rate-constant ratio (PRCR) values obtained from kinetic modelling and experiments in this work. “Overall” refers to the average error over all data used for the model.

Model	NMR peak $j$	Species modelled	# data	RMSE	MAPE	PRCR
Minimal model	6.86	<b>1</b>	20	0.0024	3.87	
	4.51	<b>2</b>	20	0.0007	0.96	
	5.14	<b>3</b>	20	0.0010	8.19	68:32
	4.40	<b>4</b>	20	0.0011	14.7	
	Overall	<b>1-4</b>	80	0.0015	6.94	
Expt.						72:28

## Tautomerisation reaction - Estimated values for $k_{C^*}$ in Acetonitrile and Methanol

Table S5: Estimated reaction-rate constants  $k_{C^*}$  ( $\text{dm}^3 \text{mol}^{-1} \text{s}^{-1}$ ) for Scheme 2 with their 95% confidence intervals (CI), obtained based on the various models developed for acetonitrile-d<sub>3</sub> and methanol-d<sub>4</sub> at 298 K.

Solvent	Model	$k_{C^*}$	95% CI
Acetonitrile-d <sub>3</sub>	Model 1+2+3	1017.2	$[0.000-9.56] \times 10^7$
	Model 1+2+3	791.5	$[0.000-8.000] \times 10^7$
Methanol-d <sub>4</sub>	Model 1+2+3+5	1000.2	$[0.000-2.190] \times 10^8$
	Model 1+2+3+4+5	1139.6	$[0.000-2.438] \times 10^8$

## Acetonitrile-d<sub>3</sub> - Arrhenius fitting and errors with Model 1+2+3

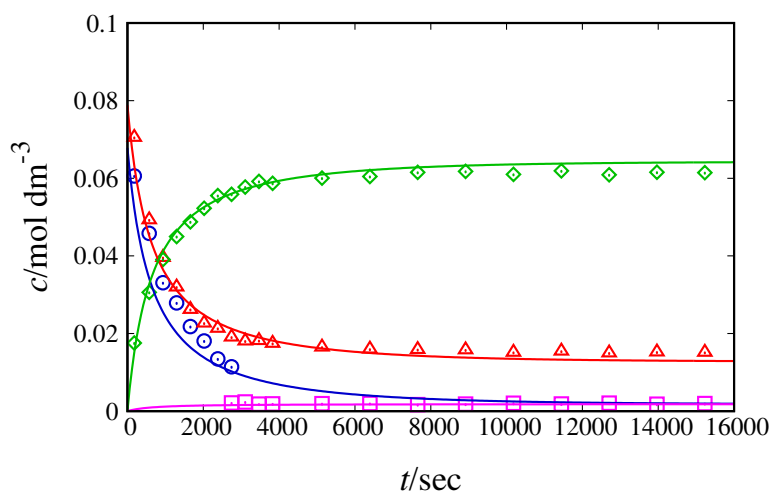


Figure S1: Experimental and Arrhenius calculated concentration profiles for reactants and products of Schemes 1-3 in acetonitrile-d<sub>3</sub> at 298 K. Continuous lines correspond to fitting with Model 1+2+3. Symbols denote experimental data. Blue circles correspond to species 1+7, red triangles to species 2, green diamonds to species 3 and pink squares to species 4+5.

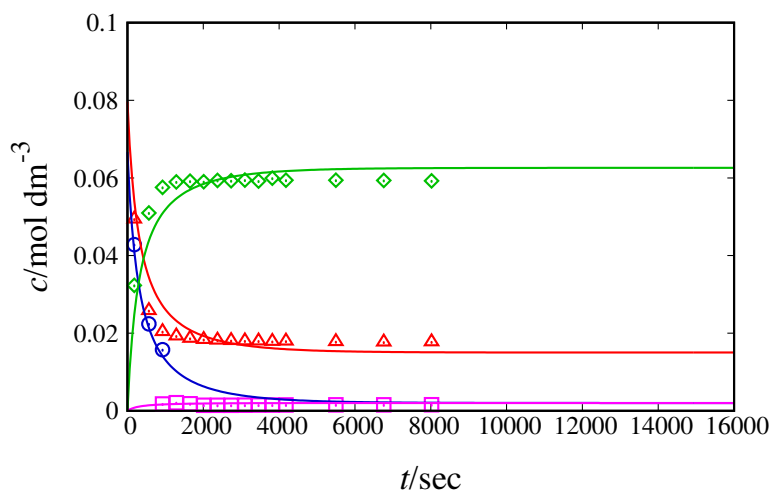


Figure S2: Experimental and Arrhenius calculated concentration profiles for reactants and products of Schemes 1-3 in acetonitrile- $d_3$  at 313 K. Continuous lines correspond to fitting with Model 1+2+3. Symbols denote experimental data. Blue circles correspond to species **1+7**, red triangles to species **2**, green diamonds to species **3** and pink squares to species **4+5**.

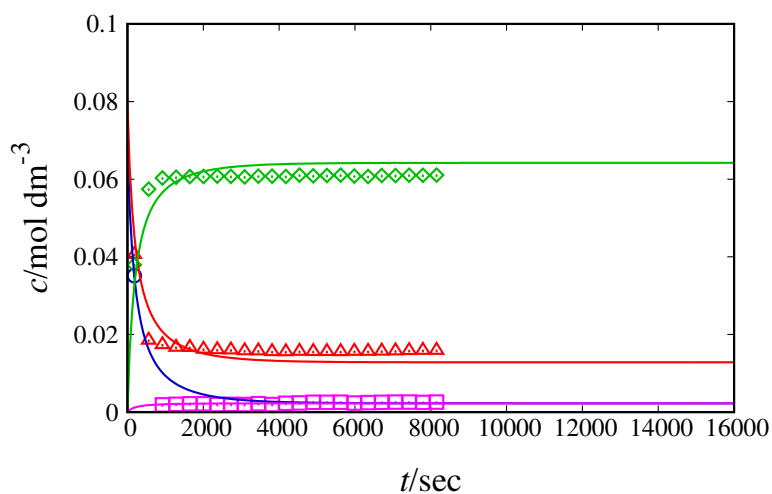


Figure S3: Experimental and Arrhenius calculated concentration profiles for reactants and products of Schemes 1-3 in acetonitrile- $d_3$  at 323 K. Continuous lines correspond to fitting with Model 1+2+3. Symbols denote experimental data. Blue circles correspond to species **1+7**, red triangles to species **2**, green diamonds to species **3** and pink squares to species **4+5**.



Table S6: Root-mean-square error (RMSE) (in mol dm<sup>-3</sup>) and mean absolute percentage error (MAPE) (in %) for all measurements in acetonitrile-d<sub>3</sub> at 298, 313 and 323 K using the Arrhenius parameters and fitted with Model 1+2+3, and percentage rate-constant ratio (PRCR) values obtained from kinetic modelling and experiments.

<i>T</i> (K)	NMR peak <i>j</i>	Species modelled	<i>N<sub>j</sub></i>	RMSE	MAPE	PRCR
298	6.79-7.05	<b>1+7</b>	8	0.0068	20.1	97:3
	4.54-4.65	<b>2</b>	20	0.0025	8.90	
	5.19-5.23	<b>3</b>	20	0.0017	3.34	
	4.36-4.47	<b>4+5</b>	13	0.0003	11.9	
	All	<b>1-5, 7</b>	61	0.0030	9.19	
313	6.79-7.05	<b>1+7</b>	3	0.0015	6.42	97:3
	4.54-4.65	<b>2</b>	15	0.0036	13.0	
	5.19-5.23	<b>3</b>	15	0.0038	6.04	
	4.36-4.47	<b>4+5</b>	13	0.0004	26.7	
	All	<b>1-5, 7</b>	46	0.0030	14.2	
323	6.79-7.05	<b>1+7</b>	1	0.0001	0.27	97:3
	4.54-4.65	<b>2</b>	10	0.0035	14.3	
	5.19-5.23	<b>3</b>	10	0.0034	5.29	
	4.36-4.47	<b>4+5</b>	8	0.0002	6.86	
	All	<b>1-5, 7</b>	29	0.0029	8.67	
All	All	<b>1-5, 7</b>	136	0.0030	10.8	
Expt.						97:3

## Acetonitrile-d<sub>3</sub> - Eyring fitting and errors with Model 1+2+3

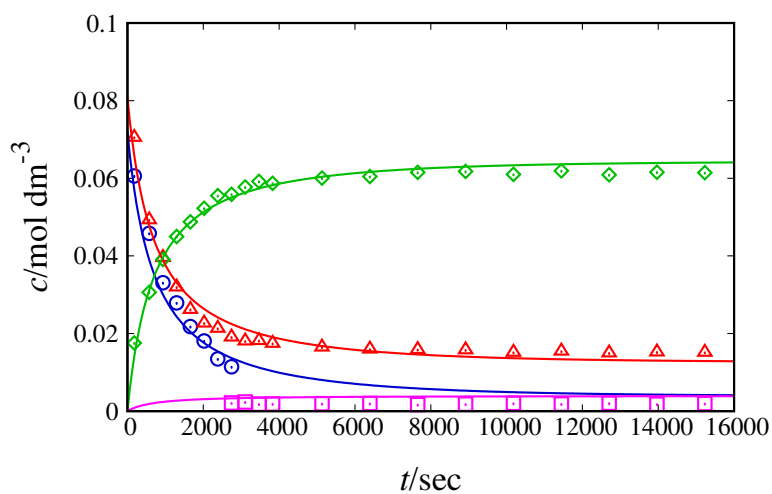


Figure S4: Experimental and Eyring calculated concentration profiles for reactants and products of Schemes 1-3 in acetonitrile-d<sub>3</sub> at 298 K. Continuous lines correspond to fitting with Model 1+3. Symbols denote experimental data. Blue circles correspond to species **1+7**, red triangles to species **2**, green diamonds to species **3** and pink squares to species **4+5**.

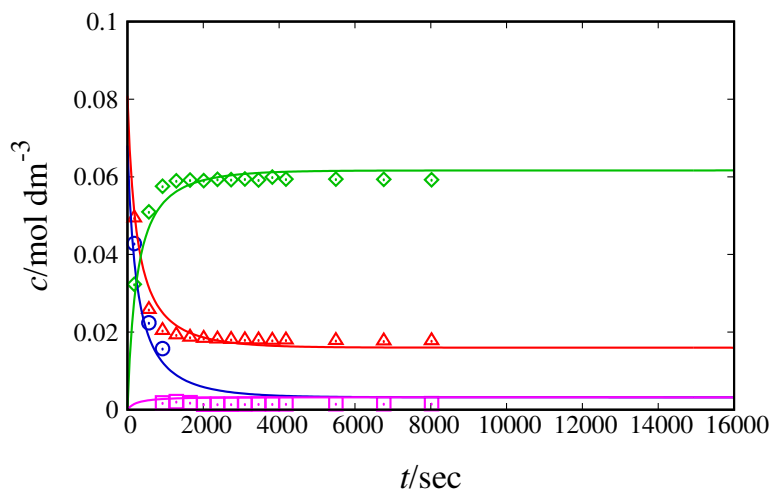


Figure S5: Experimental and Eyring calculated concentration profiles for reactants and products of Schemes 1-3 in acetonitrile- $d_3$  at 313 K. Continuous lines correspond to fitting with Model 1+3. Symbols denote experimental data. Blue circles correspond to species **1+7**, red triangles to species **2**, green diamonds to species **3** and pink squares to species **4+5**.

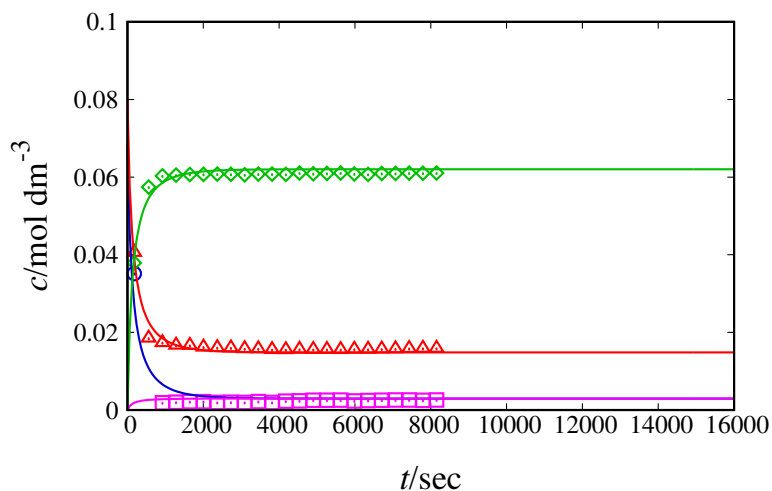


Figure S6: Experimental and Eyring calculated concentration profiles for reactants and products of Schemes 1-3 in acetonitrile- $d_3$  at 323 K. Continuous lines correspond to fitting with Model 1+3. Symbols denote experimental data. Blue circles correspond to species **1+7**, red triangles to species **2**, green diamonds to species **3** and pink squares to species **4+5**.

Table S7: Root-mean-square error (RMSE) (in mol dm<sup>-3</sup>) and mean absolute percentage error (MAPE) (in %) for all measurements in acetonitrile-d<sub>3</sub> at 298, 313 and 323 K using the Eyring parameters and fitted with Model 1+2+3, and percentage rate-constant ratio (PRCR) values obtained from kinetic modelling and experiments.

<i>T</i> (K)	NMR peak <i>j</i>	Species modelled	<i>N<sub>j</sub></i>	RMSE	MAPE	PRCR
298	6.79-7.05	<b>1+7</b>	8	0.0034	10.7	94:6
	4.54-4.65	<b>2</b>	20	0.0023	9.97	
	5.19-5.23	<b>3</b>	20	0.0017	3.10	
	4.36-4.47	<b>4+5</b>	13	0.0017	90.2	
	All	<b>1-5, 7</b>	61	0.0022	24.9	
313	6.79-7.05	<b>1+7</b>	3	0.0040	16.6	95:5
	4.54-4.65	<b>2</b>	15	0.0023	8.86	
	5.19-5.23	<b>3</b>	15	0.0024	3.97	
	4.36-4.47	<b>4+5</b>	35	0.0015	99.2	
	All	<b>1-5, 7</b>	46	0.0023	33.3	
323	6.79-7.05	<b>1+7</b>	1	0.0082	23.4	95:5
	4.54-4.65	<b>2</b>	10	0.0016	6.51	
	5.19-5.23	<b>3</b>	10	0.0014	2.10	
	4.36-4.47	<b>4+5</b>	8	0.0009	43.2	
	All	<b>1-5, 7</b>	29	0.0020	15.7	
All	All	<b>1-5, 7</b>	136	0.0022	25.8	
Expt.						97:3

## Methanol-d<sub>4</sub> - Various models fitting errors

Table S8: Root-mean-square error (RMSE) (in mol dm<sup>-3</sup>) and mean absolute percentage error (MAPE) (in %) for all measurements in methanol-d<sub>4</sub> at 298 K fitted with the various models developed, and percentage rate-constant ratio (PRCR) values obtained from kinetic modelling and experiments.

$T$ (K)	NMR peak $j$	Species modelled	$N_j$	RMSE	MAPE	PRCR
Minimal	6.86-7.05	<b>1</b>	20	0.0024	3.87	68:32
	4.51-4.55	<b>2</b>	20	0.0007	0.96	
	5.14-5.22	<b>3</b>	20	0.0010	8.19	
	4.40-4.44	<b>4</b>	20	0.0011	14.7	
	All	<b>1-4</b>	80	0.0015	6.94	
Model 1+2+3	6.86-7.05	<b>1+7</b>	20	0.0019	2.86	68:32
	4.51-4.55	<b>2</b>	20	0.0013	2.03	
	5.14-5.22	<b>3</b>	20	0.0003	2.48	
	4.40-4.44	<b>4+5</b>	20	0.0006	9.17	
	All	<b>1-5, 7</b>	80	0.0012	4.14	
Model 1+2+3+5	6.86-7.05	<b>1+7</b>	20	0.0012	1.55	75:25
	4.51-4.55	<b>2</b>	20	0.0006	0.84	
	5.14-5.22	<b>3</b>	20	0.0004	3.82	
	4.40-4.44	<b>4+5</b>	10	0.0006	19.3	
	4.41-4.44	<b>9</b>	10	0.0006	36.4	
All	<b>1-5,7-9</b>	80	0.0008	8.52		
Model 1+2+3+4+5	6.86-7.05	<b>1+7</b>	20	0.0011	1.44	73:27
	4.51-4.55	<b>2</b>	20	0.0004	0.53	
	5.14-5.22	<b>3</b>	20	0.0009	6.68	
	4.40-4.44	<b>4+5</b>	10	0.0005	17.3	
	4.41-4.44	<b>9</b>	10	0.0006	36.3	
	6.61-6.67	<b>6</b>	20	0.0001	25.3	
All	<b>1-9</b>	100	0.0007	12.1		
Expt.						72:28

## Methanol-d<sub>4</sub> - Arrhenius fitting and errors with Model 1+2+3+4+5

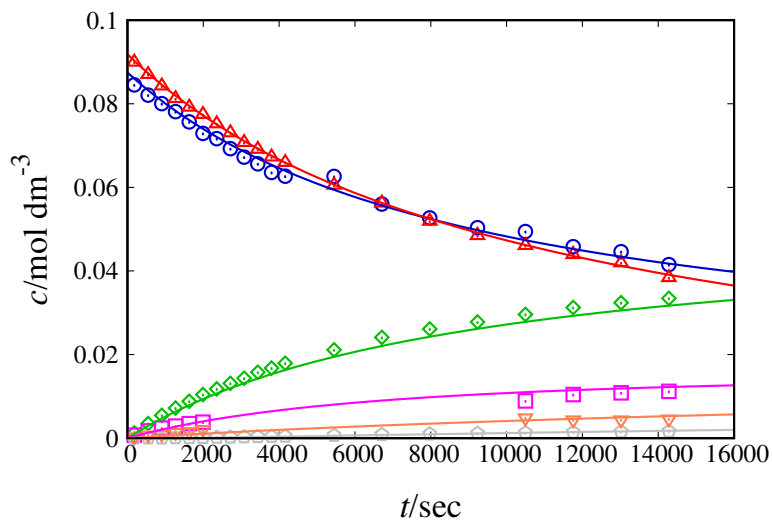


Figure S7: Experimental and Arrhenius calculated concentration profiles for reactants and products of Schemes 1-5 in methanol-d<sub>4</sub> at 298 K fitted using Model 1+2+3+4+5. Symbols denote experimental data. Blue circles correspond to species **1+7**, red triangles to species **2**, green diamonds to species **3**, pink squares to species **4+5**, orange reverse triangles to species **9** and grey pentagons to species **6**.

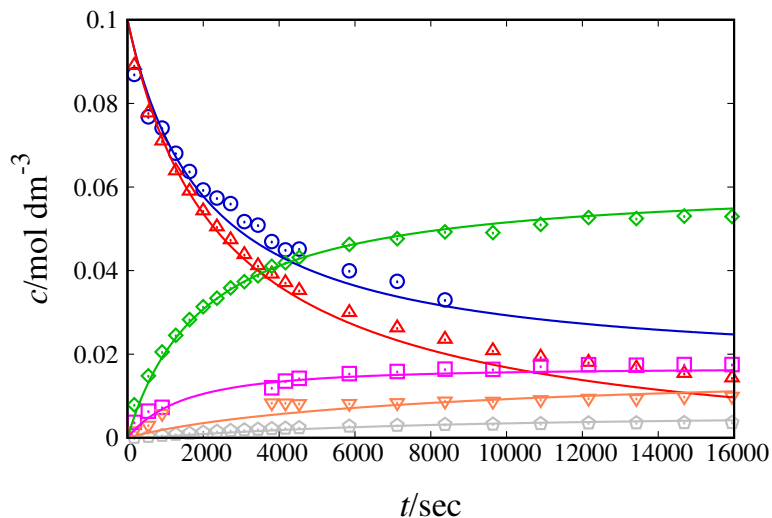


Figure S8: Experimental and Arrhenius calculated concentration profiles for reactants and products of Schemes 1-5 in methanol- $d_4$  at 313 K fitted using Model 1+2+3+4+5. Symbols denote experimental data. Blue circles correspond to species **1+7**, red triangles to species **2**, green diamonds to species **3**, pink squares to species **4+5**, orange reverse triangles to species **9** and grey pentagons to species **6**.

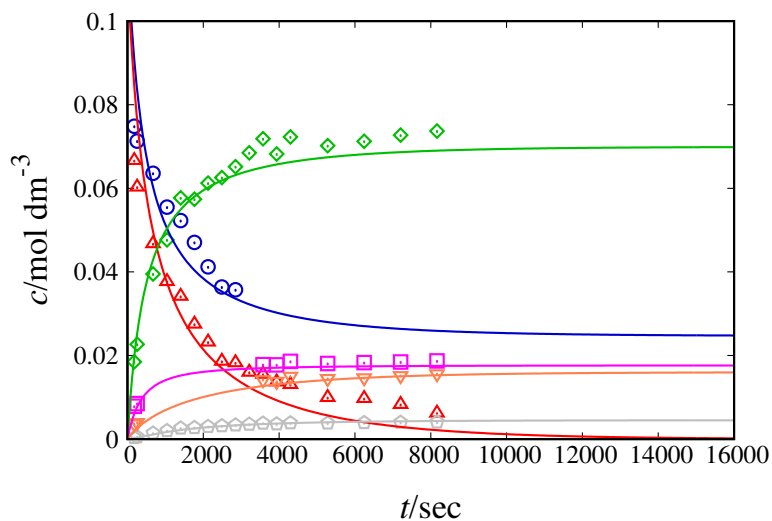


Figure S9: Experimental and Arrhenius calculated concentration profiles for reactants and products of Schemes 1-5 in methanol- $d_4$  at 328 K fitted using Model 1+2+3+4+5. Symbols denote experimental data. Blue circles correspond to species **1+7**, red triangles to species **2**, green diamonds to species **3**, pink squares to species **4+5**, orange reverse triangles to species **9** and grey pentagons to species **6**.

Table S9: Root-mean-square error (RMSE) (in mol dm<sup>-3</sup>) and mean absolute percentage error (MAPE) (in %) for all measurements in methanol-d<sub>4</sub> at 298, 313 and 328 K using the Arrhenius parameters and fitted with Model 1+2+3+4+5, and percentage rate-constant ratio (PRCR) values obtained from kinetic modelling and experiments.

$T$ (K)	NMR peak $j$	Species modelled	$N_j$	RMSE	MAPE	PRCR
298	6.86-7.05	<b>1+7</b>	20	0.0013	1.65	
	4.51-4.55	<b>2</b>	20	0.0004	0.59	
	5.14-5.22	<b>3</b>	20	0.0014	9.46	
	4.40-4.44	<b>4+5</b>	10	0.0009	14.2	69:31
	4.41-4.44	<b>9</b>	10	0.0006	36.2	
	6.61-6.67	<b>6</b>	20	0.0001	21.4	
	All	<b>1-9</b>	100	0.0009	11.7	
313	6.86-7.05	<b>1+7</b>	16	0.0034	5.64	
	4.51-4.55	<b>2</b>	23	0.0030	11.2	
	5.14-5.22	<b>3</b>	23	0.0012	3.80	
	4.40-4.44	<b>4+5</b>	16	0.0012	10.4	73:27
	4.41-4.44	<b>9</b>	16	0.0017	23.4	
	6.61-6.67	<b>6</b>	23	0.0004	23.1	
	All	<b>1-9</b>	117	0.0020	12.4	
328	6.86-7.05	<b>1+7</b>	9	0.0079	11.1	
	4.51-4.55	<b>2</b>	17	0.0069	28.4	
	5.14-5.22	<b>3</b>	17	0.0035	5.44	
	4.40-4.44	<b>4+5</b>	9	0.0011	7.71	76: 24
	4.41-4.44	<b>9</b>	9	0.0011	13.0	
	6.61-6.67	<b>6</b>	17	0.0002	11.8	
	All	<b>1-9</b>	78	0.0045	13.6	
All	All	<b>1-9</b>	295	0.0027	12.7	
Expt.						72:28



## Methanol-d<sub>4</sub> - Eyring fitting and errors with Model 1+2+3+4+5

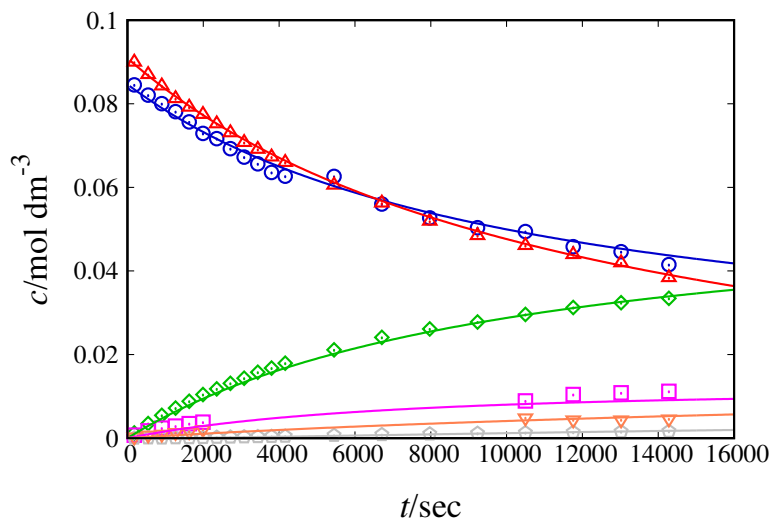


Figure S10: Experimental and Eyring calculated concentration profiles for reactants and products of Schemes 1-5 in methanol-d<sub>4</sub> at 298 K fitted using Model 1+2+3+4+5. Symbols denote experimental data. Blue circles correspond to species **1+7**, red triangles to species **2**, green diamonds to species **3**, pink squares to species **4+5**, orange reverse triangles to species **9** and grey pentagons to species **6**.

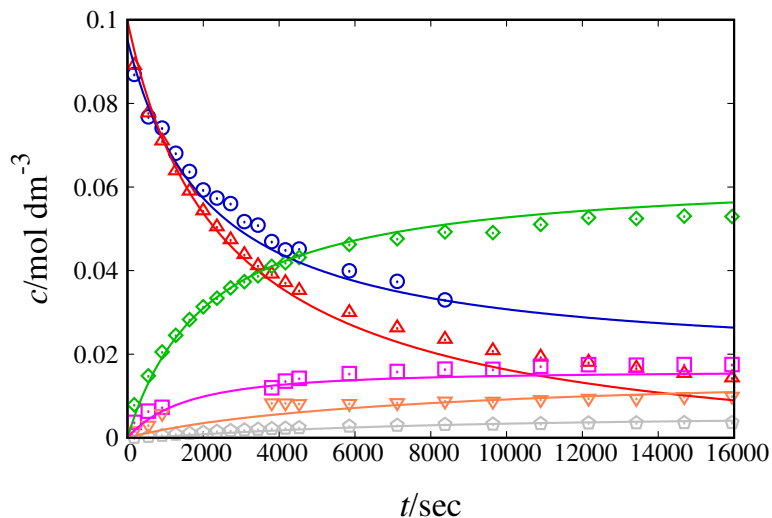


Figure S11: Experimental and Eyring calculated concentration profiles for reactants and products of Schemes 1-5 in methanol- $d_4$  at 313 K fitted using Model 1+2+3+4+5. Symbols denote experimental data. Blue circles correspond to species **1+7**, red triangles to species **2**, green diamonds to species **3**, pink squares to species **4+5**, orange reverse triangles to species **9** and grey pentagons to species **6**.

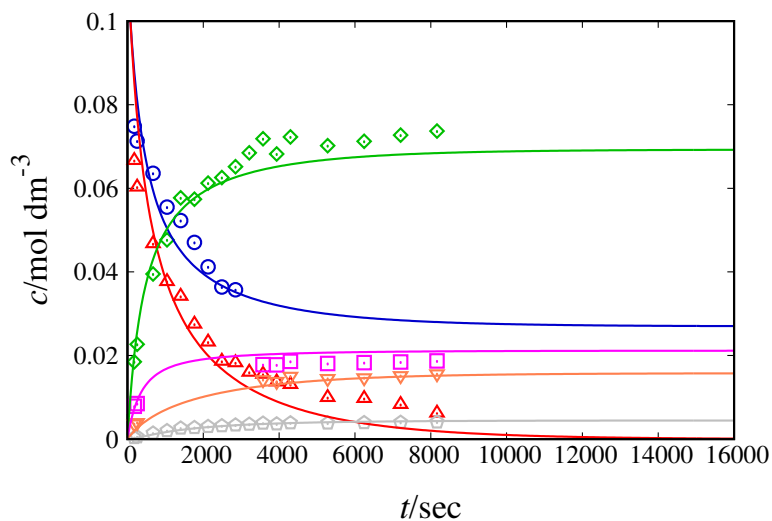


Figure S12: Experimental and Eyring calculated concentration profiles for reactants and products of Schemes 1-5 in methanol- $d_4$  at 328 K fitted using Model 1+2+3+4+5. Symbols denote experimental data. Blue circles correspond to species **1+7**, red triangles to species **2**, green diamonds to species **3**, pink squares to species **4+5**, orange reverse triangles to species **9** and grey pentagons to species **6**.

Table S10: Root-mean-square error (RMSE) (in mol dm<sup>-3</sup>) and mean absolute percentage error (MAPE) (in %) for all measurements in methanol-d<sub>4</sub> at 298, 313 and 328 K using the Eyring parameters and fitted with Model 1+2+3+4+5, and percentage rate-constant ratio (PRCR) values obtained from kinetic modelling and experiments.

<i>T</i> (K)	NMR peak <i>j</i>	Species modelled	<i>N<sub>j</sub></i>	RMSE	MAPE	PRCR
298	6.86-7.05	<b>1+7</b>	20	0.0013	1.89	
	4.51-4.55	<b>2</b>	20	0.0006	0.85	
	5.14-5.22	<b>3</b>	20	0.0008	7.01	
	4.40-4.44	<b>4+5</b>	10	0.0013	28.9	76:24
	4.41-4.44	<b>9</b>	10	0.0006	36.5	
	6.61-6.67	<b>6</b>	20	0.0001	24.8	
	All	<b>1-9</b>	100	0.0008	13.4	
313	6.86-7.05	<b>1+7</b>	16	0.0027	4.57	
	4.51-4.55	<b>2</b>	23	0.0033	12.6	
	5.14-5.22	<b>3</b>	23	0.0018	4.87	
	4.40-4.44	<b>4+5</b>	16	0.0018	14.8	74:26
	4.41-4.44	<b>9</b>	16	0.0017	23.0	
	6.61-6.67	<b>6</b>	23	0.0004	24.7	
	All	<b>1-9</b>	117	0.0021	13.6	
328	6.86-7.05	<b>1+7</b>	9	0.0066	9.01	
	4.51-4.55	<b>2</b>	17	0.0072	29.9	
	5.14-5.22	<b>3</b>	17	0.0038	6.18	
	4.40-4.44	<b>4+5</b>	9	0.0021	11.9	73:27
	4.41-4.44	<b>9</b>	9	0.0011	12.9	
	6.61-6.67	<b>6</b>	17	0.0002	11.6	
	All	<b>1-9</b>	78	0.0045	14.3	
All	All	<b>1-9</b>	295	0.0027	13.9	
Expt.						72:28

## Kinetic models

### Minimal Model

The set of differential equations that constitute the Minimal model is given as follows:

$$\frac{d[1]}{dt} = -(k_{\text{O}} + k_{\text{CM}}) \cdot [1] \cdot [2] \quad (1)$$

$$\frac{d[2]}{dt} = -(k_{\text{O}} + k_{\text{CM}}) \cdot [1] \cdot [2] \quad (2)$$

$$\frac{d[3]}{dt} = k_{\text{O}} \cdot [1] \cdot [2] \quad (3)$$

$$\frac{d[4]}{dt} = k_{\text{CM}} \cdot [1] \cdot [2] \quad (4)$$

$$[1]_{t=0} = [1]_0, [2]_{t=0} = [2]_0, [3]_{t=0} = 0, [4]_{t=0} = 0, \quad (5)$$

where  $t$  is time,  $k_{\text{O}}$  and  $k_{\text{CM}}$  (in  $\text{dm}^3 \text{mol}^{-1} \text{s}^{-1}$ ) are, respectively, the rate constants for the formation of the O-alkylated product and the C-alkylated product,  $[i]_{t=0}$  is the initial concentration of component  $i = 1, 2, 3$  and 4, as specified in Scheme1 1-3 at time zero.

### Model 1+2+3+4+5

For the reaction kinetics in methanol- $d_4$ , the more detailed Model 1+2+3+4+5 is necessary to be applied, as it describes more accurately the relevant mechanism features in this solvent. Additionally to the kinetics for the formation of the two main products following Schemes 1-3, Model 1+2+3+4+5 includes the double alkylation reaction (Scheme 4) and the kinetics of the reaction between benzyl bromide with methanol- $d_4$  (Scheme 5). The set of differential equations that constitute Model 1+2+3+4+5 is given as follows:

$$\frac{d[1]}{dt} = -(k_{\text{O}} + k_{\text{C}}) \cdot [1] \cdot [2] - k_{\text{C}^*} \cdot [1] \cdot [4^*] + k_f \cdot [5] \cdot [7] - k_r \cdot [1] \cdot [4] \quad (6)$$

$$\frac{d[2]}{dt} = -(k_O + k_C) \cdot [1] \cdot [2] - k_{\text{BME}} \cdot [2] \cdot [8] - k_{\text{DC}} \cdot [2] \cdot [5] \quad (7)$$

$$\frac{d[3]}{dt} = k_O \cdot [1] \cdot [2] \quad (8)$$

$$\frac{d[4^*]}{dt} = k_C \cdot [1] \cdot [2] - k_{C^*} \cdot [1] \cdot [4^*] \quad (9)$$

$$\frac{d[4]}{dt} = k_f \cdot [5] \cdot [7] - k_r \cdot [1] \cdot [4] \quad (10)$$

$$\frac{d[5]}{dt} = k_{C^*} \cdot [1] \cdot [4^*] - k_f \cdot [5] \cdot [7] + k_r \cdot [1] \cdot [4] - k_{\text{DC}} \cdot [2] \cdot [5] \quad (11)$$

$$\frac{d[6]}{dt} = k_{\text{DC}} \cdot [2] \cdot [5] \quad (12)$$

$$\frac{d[7]}{dt} = -k_{C^*} \cdot [1] \cdot [4^*] - k_f \cdot [5] \cdot [7] + k_r \cdot [1] \cdot [4] \quad (13)$$

$$\frac{d[9]}{dt} = k_{\text{BME}} \cdot [2] \cdot [8] \quad (14)$$

$$K_{\text{eq}} = \frac{k_f}{k_r} \quad (15)$$

$$[\text{Sum}_1] = [1] + [7] \quad (16)$$

$$[\text{Sum}_2] = [4] + [5] \quad (17)$$

$$\begin{aligned}
[1]_{t=0} &= [1]_0, [2]_{t=0} = [2]_0, [3]_{t=0} = 0, [4^*]_{t=0} = 0, [4]_{t=0} = 0, [6]_{t=0} = 0, \\
[7]_{t=0} &= 0, [8]_{t=0} = [8]_0, [9]_{t=0} = 0,
\end{aligned} \tag{18}$$

where  $t$  is time,  $k_O$  and  $k_{CM}$  (in  $\text{dm}^3 \text{mol}^{-1} \text{s}^{-1}$ ) are, respectively, the rate constants for the formation of the O-alkylated product and the keto tautomer of the C-alkylated product,  $k_{DC}$  ( $\text{dm}^3 \text{mol}^{-1} \text{s}^{-1}$ ) is the rate constant for the formation of the double C-alkylated product,  $k_{BME}$  ( $\text{dm}^3 \text{mol}^{-1} \text{s}^{-1}$ ) is the rate constant for the formation of benzyl methyl ether,  $K_{eq}$  is the equilibrium constant,  $k_f$  and  $k_r$  ( $\text{dm}^3 \text{mol}^{-1} \text{s}^{-1}$ ) are, respectively, the rate constants for the forward and the reverse reaction of Scheme 3,  $[\text{Sum}_1]$  (referred here as ‘‘total naphthol’’) is the sum of the concentrations of the protonated ([7]) and deprotonated ([1]) forms of sodium  $\beta$ -naphthoxide,  $[\text{Sum}_2]$  (referred here as ‘‘total C-alkylated product’’) is the sum of concentrations of the protonated ([4]) and deprotonated ([5]) forms of the C-alkylated product and  $[i]_{t=0}$  is the initial concentration of component  $i = 1, 2, 3, 4^*, 4, 5, 6, 7, 8$  and  $9$ , as specified in Schemes 1, 2, 3, 4 and 5 at time zero. The concentration of methanol- $\text{d}_4$  at time zero,  $[8]_0$ , may be assumed to be roughly equal to the molar density of methanol- $\text{d}_4$  at the specific temperature of the experiment. As this value is significantly larger than the value of  $k_{BME}$  and it is practically invariant throughout an experiment, we may reasonably assume that the term  $k_{BME} \cdot [8]$  remains constant for an experiment at a given temperature. Temperature-dependent data for the density of methanol- $\text{d}_4$  are reported in the literature<sup>2</sup> at 298 K ( $888.11 \text{ Kg m}^{-3}$ ), but not at 313 K and 328 K. Thus, we report in our study the value for  $k_{BME} \cdot [8]$ .

## Parameter estimation in gPROMS

The maximum log likelihood objective function ( $\Phi$ ) is implemented in gPROMS as follows<sup>3</sup>

$$\Phi = \frac{N}{2} \ln(2\pi) + \frac{1}{2} \min_{\theta} \left\{ \sum_{i=1}^{NE} \sum_{j=1}^{NP_i} \sum_{l=1}^{NM_{ij}} \left[ \ln(\sigma_{ijl}^2) + \frac{(\tilde{z}_{ijk} - z_{ijl})^2}{\sigma_{ijl}^2} \right] \right\}, \tag{19}$$

where  $N$  is the total number of measurements,  $\theta$  the set of model parameters,  $NE$  the number of experiments,  $NP_i$  the number of peaks measured in each experiment  $i$ ,  $NM_{ij}$  the number of data (time) points for each peak  $j$  in each experiment  $i$ ,  $\tilde{z}_{ijl}$  the  $l$  measured concentration value for peak  $j$  in experiment  $i$ ,  $z_{ijl}$  the  $l$  model estimated concentration value for peak  $j$  in experiment  $i$ , and  $\sigma_{ijl}$  the standard deviation for the  $l$  concentration measurement obtained for peak  $j$  in experiment  $i$ .

## Electronic structure calculations - Optimized geometries

### Vacuum

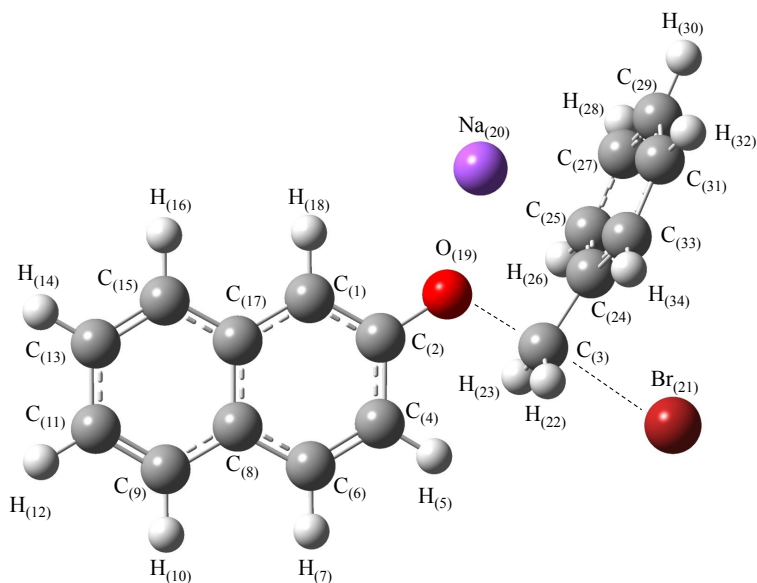


Figure S13: A transition-state structure ( $TS_{O1}$ ) for the O-alkylation pathway optimized at the B3LYP/6-31+G(d) level of theory in vacuum. The optimized values for the bond lengths, bond angles and dihedral angles are reported in Table S11.



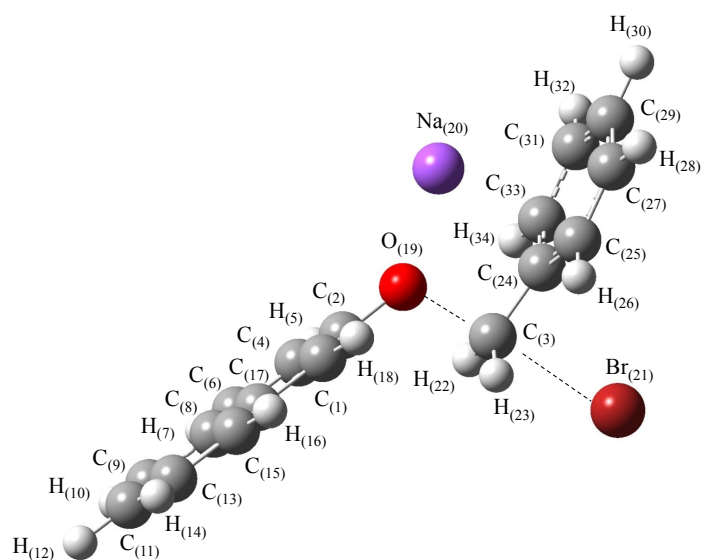


Figure S14: A transition-state structure ( $\text{TS}_{\text{O}_2}$ ) for the O-alkylation pathway optimized at the B3LYP/6-31+G(d) level of theory in vacuum. The optimized values for the bond lengths, bond angles and dihedral angles are reported in Table S12.

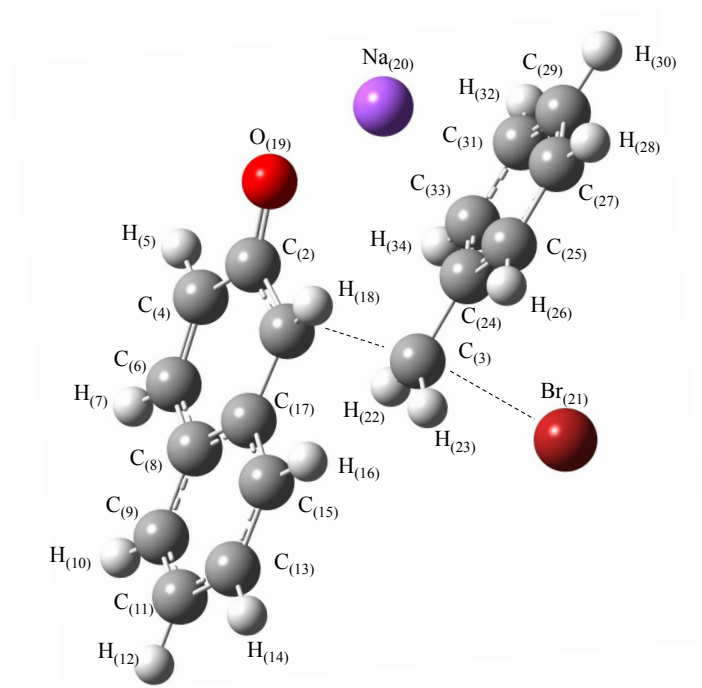


Figure S15: A transition-state structure for the C-alkylation pathway ( $TS_C$ ) optimized at the B3LYP/6-31+G(d) level of theory in vacuum. The optimized values for the bond lengths, bond angles and dihedral angles are reported in Table S13.

Table S11: Internal coordinates (Z-matrix) of the transition-state structure (TS<sub>O1</sub>) for the O-alkylation pathway optimized at the B3LYP/6-31+G(d) level of theory in vacuum. The internal coordinates for each atom are defined by the bond lengths, bond angles and dihedral angles with respect to previously defined atoms listed in columns NA (for the bond length), NB (for the bond angle) and NC (for the dihedral angle).

Atom	Symbol	NA	Bond length/Å	NB	Bond angle/°	NC	Dihedral angle/°
1	C						
2	C	1	1.3919112				
3	C	2	2.8041261	1	155.0597498		
4	C	2	1.4294120	1	118.3099253	3	-179.9974010
5	H	4	1.0844401	2	120.0241580	1	-179.9978025
6	C	4	1.3771181	2	120.6606263	5	179.9980653
7	H	6	1.0881035	4	119.3481522	2	-179.9997075
8	C	6	1.4202779	4	121.8195585	2	0.0000000
9	C	8	1.4209886	6	122.6750889	4	180.0000000
10	H	9	1.0882004	8	118.6755876	6	-0.0003237
11	C	9	1.3789488	8	120.9531268	6	179.9995695
12	H	11	1.0867756	9	120.3165963	8	180.0000000
13	C	11	1.4186228	9	119.8531872	8	0.0000000
14	H	13	1.0873936	11	119.5545023	9	-180.0000000
15	C	13	1.3786611	11	120.5783542	9	0.0000000
16	H	15	1.0885244	13	120.1789389	11	-180.0000000
17	C	15	1.4246904	13	120.9613782	11	0.0000000
18	H	1	1.0905111	2	119.3598443	4	179.9996242
19	O	2	1.3485949	1	119.4767799	17	179.9997352
20	Na	19	2.1668064	2	137.0364750	1	-0.0041178
21	Br	19	4.4694823	2	118.5275655	1	-179.9988661
22	H	3	1.0771025	19	95.5711050	2	-59.7111134
23	H	3	1.0771025	19	95.5717490	2	59.7021782
24	C	3	1.4719024	19	5.3128574	2	179.9954623
25	C	24	1.4091966	3	20.2355092	19	-84.4390017
26	H	25	1.0866947	24	19.1251296	3	-11.9889916
27	C	25	1.3978789	24	20.6675265	3	168.5994838
28	H	27	1.0871672	25	19.6630137	24	178.9568530
29	C	27	1.4032979	25	20.3624604	24	-0.2506517
30	H	29	1.0865032	27	20.3305098	25	179.4388620
31	C	29	1.4032981	27	19.3213442	25	0.9578473
32	H	31	1.0871665	29	19.9696893	27	178.2471632
33	C	31	1.3978791	29	120.3624602	27	-0.9577451
34	H	33	1.0866951	31	120.2046817	29	179.6554902

Table S12: Internal coordinates (Z-matrix) of the transition-state structure (TS<sub>O2</sub>) for the O-alkylation pathway optimized at the B3LYP/6-31+G(d) level of theory in vacuum. The internal coordinates for each atom are defined by the bond lengths, bond angles and dihedral angles with respect to previously defined atoms listed in columns NA (for the bond length), NB (for the bond angle) and NC (for the dihedral angle).

Atom	Symbol	NA	Bond length/Å	NB	Bond angle/°	NC	Dihedral angle/°
1	C						
2	C	1	1.3867285				
3	C	2	2.7122776	1	119.9934426		
4	C	2	1.4277180	1	119.2041693	3	135.1140135
5	H	4	1.0871891	2	118.5635966	1	-179.7079005
6	C	4	1.3757901	2	120.6465003	5	-179.3785902
7	H	6	1.0881689	4	120.0018313	2	179.7617867
8	C	6	1.4231519	4	121.2120855	2	-0.2467762
9	C	8	1.4208294	6	122.4178738	4	-179.9590674
10	H	9	1.0881511	8	118.7318122	6	-0.0753447
11	C	9	1.3792964	8	120.9315648	6	179.8415835
12	H	11	1.0868703	9	120.2047895	8	-179.9176264
13	C	11	1.4179447	9	120.0216095	8	-0.1349361
14	H	13	1.0871967	11	119.6044698	9	-179.7872054
15	C	13	1.3789642	11	120.4386191	9	0.0341126
16	H	15	1.0881088	13	120.2768118	11	-179.7174583
17	C	15	1.4234583	13	120.9326915	11	0.0195397
18	H	1	1.0882919	2	119.2027373	4	179.0543634
19	O	2	1.3555944	1	121.1094302	17	178.4653772
20	Na	19	2.1464896	2	143.0010806	1	-75.6351528
21	Br	19	4.4921722	2	113.1922307	1	100.4346619
22	H	3	1.0782637	19	96.4347805	2	61.9500182
23	H	3	1.0788936	19	95.7521488	2	-56.5337286
24	C	3	1.4707169	19	96.6572925	2	-177.2859305
25	C	24	1.4103247	3	120.1810485	19	83.3756715
26	H	25	1.0866764	24	119.0289506	3	13.6681249
27	C	25	1.3975455	24	120.7619358	3	-167.1904167
28	H	27	1.0872665	25	119.6403491	24	-178.8370651
29	C	27	1.4034866	25	120.4128109	24	0.3979701
30	H	29	1.0864959	27	120.3696616	25	-179.4952207
31	C	29	1.4032416	27	119.2386830	25	-1.0240064
32	H	31	1.0872602	29	119.9556563	27	-178.2051968
33	C	31	1.3977982	29	120.3979788	27	0.9530106
34	H	33	1.0866964	31	120.1681531	29	-179.4096836

Table S13: Internal coordinates (Z-matrix) of the transition-state structure for the C-alkylation pathway (TS<sub>C</sub>) optimized at the B3LYP/6-31+G(d) level of theory in vacuum. The internal coordinates for each atom are defined by the bond lengths, bond angles and dihedral angles with respect to previously defined atoms listed in columns NA (for the bond length), NB (for the bond angle) and NC (for the dihedral angle).

Atom	Symbol	NA	Bond length/Å	NB	Bond angle/°	NC	Dihedral angle/°
1	C						
2	C	1	1.4416769				
3	C	2	2.8502086	1	48.0616595		
4	C	2	1.4511836	1	116.8793163	3	91.0506127
5	H	4	1.0866673	2	117.3245749	1	-173.0780333
6	C	4	1.3646970	2	121.1549917	5	-177.0228568
7	H	6	1.0889378	4	119.7371446	2	178.4108872
8	C	6	1.4398436	4	122.2885719	2	0.2954098
9	C	8	1.4117717	6	121.9360897	4	175.6030173
10	H	9	1.0880984	8	118.9558474	6	1.9772553
11	C	9	1.3868267	8	120.7904048	6	-177.7774664
12	H	11	1.0864638	9	120.2782633	8	-179.9378714
13	C	11	1.4075504	9	119.6167661	8	0.0402577
14	H	13	1.0870223	11	119.8085445	9	179.7384100
15	C	13	1.3887162	11	120.4626048	9	-0.4637753
16	H	15	1.0884469	13	119.8157671	11	-179.7975018
17	C	15	1.4108797	13	120.9308695	11	0.2257012
18	H	1	1.0890101	2	115.8161714	4	-166.8295753
19	O	2	1.2756710	1	122.5475164	17	164.7499936
20	Na	19	2.1018148	2	134.7395568	1	40.3082881
21	Br	19	5.9349912	2	59.6890533	1	62.1643513
22	H	3	1.0783710	19	92.7438496	2	52.3624494
23	H	3	1.0774315	19	125.1196082	2	-74.5395508
24	C	3	1.4655427	19	69.7576345	2	173.1997621
25	C	24	1.4108360	3	120.9231529	19	103.5471723
26	H	25	1.0869639	24	119.2416733	3	2.4671096
27	C	25	1.3984220	24	121.0388925	3	179.9326884
28	H	27	1.0873268	25	119.6658224	24	-177.6664261
29	C	27	1.4051896	25	120.3037785	24	0.2725979
30	H	29	1.0868505	27	120.3931495	25	-177.4345972
31	C	29	1.4057901	27	119.1347343	25	0.5501858
32	H	31	1.0871800	29	119.9715522	27	-178.7780047
33	C	31	1.3965275	29	120.4069796	27	-0.0575287
34	H	33	1.0857936	31	119.8535811	29	-178.7241123

## Acetonitrile

Table S14: Internal coordinates (Z-matrix) of the transition-state structure (TS<sub>O2</sub>) for the O-alkylation pathway optimized at the B3LYP/6-31+G(d) level of theory in acetonitrile. The internal coordinates for each atom are defined by the bond lengths, bond angles and dihedral angles with respect to previously defined atoms listed in columns NA (for the bond length), NB (for the bond angle) and NC (for the dihedral angle).

Atom	Symbol	NA	Bond length/Å	NB	Bond angle/°	NC	Dihedral angle/°
1	C						
2	C	1	1.3953836				
3	C	2	2.8507099	1	126.9074237		
4	C	2	1.4358900	1	118.2254153	3	-130.1878021
5	H	4	1.0876090	2	118.3083413	1	179.8587484
6	C	4	1.3760120	2	121.2296797	5	179.4606934
7	H	6	1.0886672	4	120.0515585	2	-179.7130808
8	C	6	1.4251923	4	121.2229164	2	-0.0398753
9	C	8	1.4217558	6	122.4310089	4	-179.9710062
10	H	9	1.0885682	8	118.6738398	6	0.1897951
11	C	9	1.3816025	8	120.9230686	6	-179.8328042
12	H	11	1.0872529	9	120.2785917	8	-179.9855636
13	C	11	1.4195740	9	119.9170332	8	0.0252948
14	H	13	1.0876720	11	119.5688198	9	-179.9599986
15	C	13	1.3807984	11	120.5300722	9	0.0445225
16	H	15	1.0883779	13	120.2906093	11	179.9467167
17	C	15	1.4264509	13	120.9781146	11	0.0562042
18	H	1	1.0887846	2	119.0718063	4	-179.4632667
19	O	2	1.3339834	1	121.7213302	17	-178.6219468
20	Na	19	2.1653373	2	141.8084819	1	48.4939097
21	Br	19	4.6188256	2	107.8389103	1	-112.4519885
22	H	3	1.0765245	19	89.9004133	2	-70.7626541
23	H	3	1.0776392	19	89.4127843	2	48.3304400
24	C	3	1.4613242	19	94.5001509	2	168.6609558
25	C	24	1.4086402	3	120.1635055	19	-86.8028089
26	H	25	1.0871050	24	119.4447374	3	-6.2016110
27	C	25	1.3970892	24	120.3775220	3	172.8942017
28	H	27	1.0867476	25	119.8011556	24	-179.6521615
29	C	27	1.4025529	25	120.1382447	24	0.1130743
30	H	29	1.0866409	27	120.0910463	25	-179.5902726
31	C	29	1.4018692	27	119.8041336	25	0.2125367
32	H	31	1.0867763	29	120.0538440	27	-179.9522467
33	C	31	1.3978134	29	120.1645560	27	-0.1948010
34	H	33	1.0870746	31	120.1365776	29	-179.1997541

Table S15: Internal coordinates (Z-matrix) of the transition-state structure for the C-alkylation pathway (TS<sub>C</sub>) optimized at the B3LYP/6-31+G(d) level of theory in acetonitrile. The internal coordinates for each atom are defined by the bond lengths, bond angles and dihedral angles with respect to previously defined atoms listed in columns NA (for the bond length), NB (for the bond angle) and NC (for the dihedral angle).

Atom	Symbol	NA	Bond length/Å	NB	Bond angle/°	NC	Dihedral angle/°
1	C						
2	C	1	1.4320595				
3	C	2	2.9254022	1	52.9464326		
4	C	2	1.4537565	1	116.7399712	3	91.9818680
5	H	4	1.0877151	2	117.4981175	1	-174.6342753
6	C	4	1.3662183	2	121.5377147	5	-177.8660884
7	H	6	1.0889624	4	119.9808522	2	178.6377077
8	C	6	1.4385424	4	121.9172720	2	-0.0044167
9	C	8	1.4142405	6	121.9816262	4	176.6948981
10	H	9	1.0883685	8	118.8224315	6	1.3296750
11	C	9	1.3876070	8	120.8009337	6	-178.3593153
12	H	11	1.0870570	9	120.2897959	8	179.8680702
13	C	11	1.4116930	9	119.6521347	8	0.0548517
14	H	13	1.0876375	11	119.7022686	9	179.5708436
15	C	13	1.3880507	11	120.5361378	9	-0.3936047
16	H	15	1.0882788	13	120.0669515	11	-179.9026130
17	C	15	1.4170749	13	120.9138720	11	0.2186015
18	H	1	1.0877168	2	117.6307877	4	-171.8673509
19	O	2	1.2803858	1	122.8723359	17	168.3818662
20	Na	19	2.1458781	2	136.1151809	1	26.7201239
21	Br	19	6.0265338	2	58.9589076	1	66.7596573
22	H	3	1.0778827	19	86.7973659	2	53.1418620
23	H	3	1.0771221	19	120.7022425	2	-68.8481425
24	C	3	1.4503847	19	68.2917435	2	178.2250249
25	C	24	1.4122383	3	120.4331236	19	108.5323415
26	H	25	1.0870079	24	119.3966720	3	0.0677749
27	C	25	1.3960420	24	120.6219779	3	-179.8697897
28	H	27	1.0867348	25	119.8842496	24	-179.8884167
29	C	27	1.4062008	25	120.1404256	24	-0.5285928
30	H	29	1.0867809	27	120.1145569	25	-179.2876519
31	C	29	1.4034162	27	119.6889803	25	0.8706417
32	H	31	1.0867347	29	120.0184594	27	179.6343280
33	C	31	1.3975863	29	120.1494251	27	-0.2062842
34	H	33	1.0863207	31	119.8927212	29	179.7777906

## Methanol

Table S16: Internal coordinates (Z-matrix) of the transition-state structure (TS<sub>O2</sub>) for the O-alkylation pathway optimized at the B3LYP/6-31+G(d) level of theory in methanol. The internal coordinates for each atom are defined by the bond lengths, bond angles and dihedral angles with respect to previously defined atoms listed in columns NA (for the bond length), NB (for the bond angle) and NC (for the dihedral angle).

Atom	Symbol	NA	Bond length/Å	NB	Bond angle/°	NC	Dihedral angle/°
1	C						
2	C	1	1.3937507				
3	C	2	2.8388448	1	124.3560486		
4	C	2	1.4343640	1	118.4260526	3	130.5504888
5	H	4	1.0878192	2	118.3833455	1	179.9595188
6	C	4	1.3759443	2	121.1438711	5	-179.1642994
7	H	6	1.0886855	4	120.0182597	2	179.6239175
8	C	6	1.4248928	4	121.1963617	2	-0.0808315
9	C	8	1.4217183	6	122.4202841	4	179.9367642
10	H	9	1.0886239	8	118.7241810	6	-0.0885062
11	C	9	1.3813087	8	120.8991490	6	179.9480615
12	H	11	1.0873872	9	120.2598666	8	179.9757999
13	C	11	1.4193074	9	119.9526020	8	-0.0347389
14	H	13	1.0877633	11	119.5776307	9	179.9595056
15	C	13	1.3805602	11	120.5235213	9	-0.0462172
16	H	15	1.0884512	13	120.2703076	11	-179.9470922
17	C	15	1.4260012	13	120.9509934	11	-0.0285512
18	H	1	1.0888471	2	119.1806467	4	179.4634030
19	O	2	1.3389537	1	121.6910229	17	178.6825316
20	Na	19	2.1762890	2	141.2293399	1	-47.7295776
21	Br	19	4.6224105	2	107.5626673	1	108.7879830
22	H	3	1.0769285	19	90.1655322	2	71.4468007
23	H	3	1.0780742	19	90.0834058	2	-47.5085939
24	C	3	1.4611887	19	94.8886208	2	-167.8557454
25	C	24	1.4088030	3	120.1044305	19	88.0331897
26	H	25	1.0872251	24	119.4815837	3	6.4815024
27	C	25	1.3968899	24	120.3750842	3	-172.7931126
28	H	27	1.0868710	25	119.8083878	24	179.7294314
29	C	27	1.4024788	25	120.1325914	24	-0.0982448
30	H	29	1.0867565	27	120.0964682	25	179.6053988
31	C	29	1.4016497	27	119.8142379	25	-0.1861974
32	H	31	1.0869035	29	120.0543154	27	179.8979760
33	C	31	1.3977188	29	120.1708978	27	0.1790437
34	H	33	1.0871797	31	120.1231179	29	179.1581307



Table S17: Internal coordinates (Z-matrix) of the transition-state structure for the C-alkylation pathway (TS<sub>C</sub>) optimized at the B3LYP/6-31+G(d) level of theory in methanol. The internal coordinates for each atom are defined by the bond lengths, bond angles and dihedral angles with respect to previously defined atoms listed in columns NA (for the bond length), NB (for the bond angle) and NC (for the dihedral angle).

Atom	Symbol	NA	Bond length/Å	NB	Bond angle/°	NC	Dihedral angle/°
1	C						
2	C	1	1.4298897				
3	C	2	2.9037743	1	52.4786386		
4	C	2	1.4499960	1	117.0897101	3	92.1330051
5	H	4	1.0878347	2	117.6500139	1	-174.6126569
6	C	4	1.3665694	2	121.3862758	5	-177.7587447
7	H	6	1.0888538	4	119.9009377	2	178.5888436
8	C	6	1.4376908	4	121.9183871	2	0.0315575
9	C	8	1.4143742	6	121.9482694	4	176.5763170
10	H	9	1.0883473	8	118.8686209	6	1.3587648
11	C	9	1.3870863	8	120.7442169	6	-178.3269406
12	H	11	1.0871435	9	120.2660857	8	179.8894670
13	C	11	1.4113281	9	119.6927626	8	0.0576926
14	H	13	1.0876765	11	119.7095393	9	179.5664947
15	C	13	1.3880246	11	120.5377736	9	-0.3660444
16	H	15	1.0882736	13	120.0358647	11	-179.9426758
17	C	15	1.4160261	13	120.8577622	11	0.1839036
18	H	1	1.0876735	2	117.6445429	4	-171.1452592
19	O	2	1.2873442	1	122.6724352	17	168.1374437
20	Na	19	2.1599451	2	135.1434195	1	25.5922591
21	Br	19	6.0290158	2	58.9110334	1	66.4290525
22	H	3	1.0781684	19	87.2619032	2	53.8936851
23	H	3	1.0773708	19	121.8450060	2	-68.6751174
24	C	3	1.4510934	19	68.7091638	2	178.5514623
25	C	24	1.4120473	3	120.3862529	19	108.2442682
26	H	25	1.0870860	24	119.4352934	3	0.3929888
27	C	25	1.3960710	24	120.6237827	3	-179.6103397
28	H	27	1.0868503	25	119.8857369	24	-179.8360755
29	C	27	1.4060768	25	120.1297425	24	-0.4825969
30	H	29	1.0868975	27	120.1167236	25	-179.3126089
31	C	29	1.4033148	27	119.6887694	25	0.8696727
32	H	31	1.0868160	29	120.0122773	27	179.6160001
33	C	31	1.3975337	29	120.1646095	27	-0.2324260
34	H	33	1.0864937	31	119.8649719	29	179.8270162

Table S18: QM-calculated imaginary frequency of the transition-state structure ( $\nu^\ddagger$ ), ideal-gas electronic energy ( $\underline{E}^{\text{el,IG}}$ ), zero-point vibrational energy (ZPVE) and ideal-gas molecular partition function at 298 K ( $q'^{\text{IG}}(298)$ ) of the transition-state structures for both the alkylation pathways optimized at the B3LYP/6-31+G(d) level of theory in vacuum. For the O-alkylation pathway, only the transition-state structure TS 2 is considered.

Structure	$\nu^\ddagger/\text{cm}^{-1}$	$\underline{E}^{\text{el,IG}}/\text{a.u. Particle}^{-1}$	ZPVE/a.u. Particle $^{-1}$	$q'^{\text{IG}}(298)$
TS <sub>O2</sub>	-391.82	-3465.548177	0.250160	2.8725E-92
TS <sub>C</sub>	-404.20	-3465.548515	0.250206	2.4206E-93

Table S19: QM-calculated imaginary frequency of the transition-state structure ( $\nu^\ddagger$ ), liquid-phase electronic energy ( $\underline{E}^{\text{el,L}}$ ), zero-point vibrational energy (ZPVE) and the non-electrostatic term of the solvation free energy ( $\underline{G}^{\text{CDS,L}}$ ) at 298 K of the transition-state structures for the O-alkylation and C-alkylation pathways optimized at the B3LYP/6-31+G(d) level of theory in acetonitrile and methanol.

Solvent	Structure	$\nu^\ddagger/\text{cm}^{-1}$	$\underline{E}^{\text{el,L}}/\text{a.u. Particle}^{-1}$	ZPVE/a.u. Particle $^{-1}$	$\underline{G}^{\text{CDS,L}}/\text{kcal mol}^{-1}$
Acetonitrile	TS <sub>O2</sub>	-396.59	-3465.599236	0.249584	-5.08
	TS <sub>C</sub>	-360.75	-3465.597841	0.249588	-4.98
Methanol	TS <sub>O2</sub>	-399.63	-3465.597292	0.249766	-3.24
	TS <sub>C</sub>	-371.93	-3465.597689	0.249688	-2.89

## QM-calculated free-energies of solvation ( $\Delta G^{\circ, \text{solv}}$ )

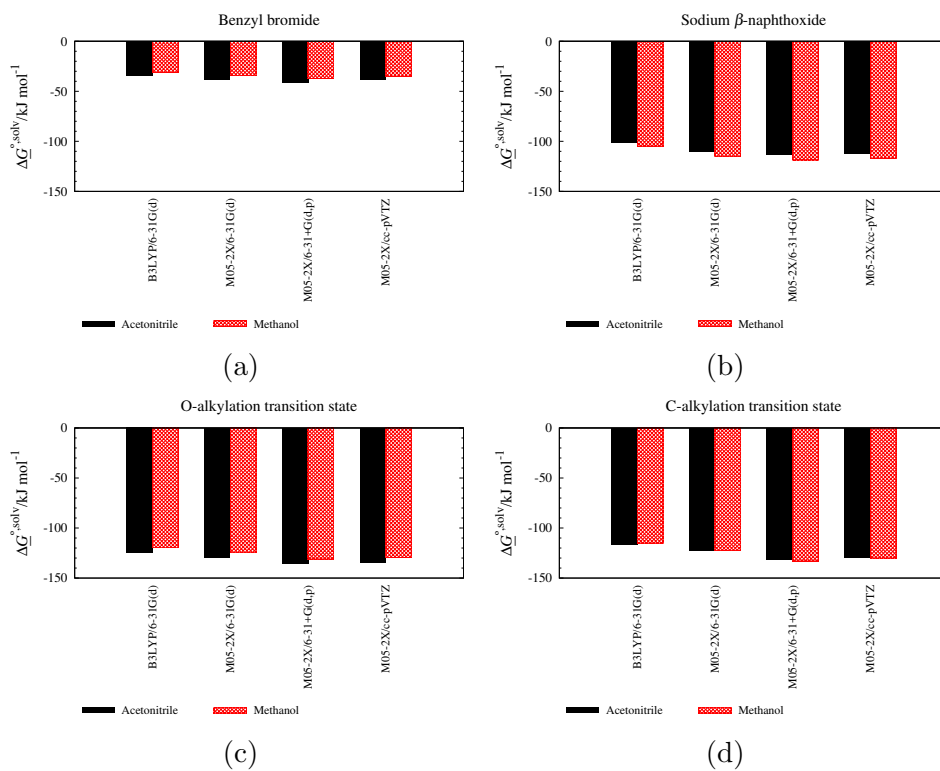


Figure S16: Free-energy of solvation in solvents acetonitrile and methanol of reaction species (a) sodium  $\beta$ -naphthoxide, (b) benzyl bromide, (c) O-alkylation transition state and (d) C-alkylation transition state using different levels of theory.

## QM-calculated values in acetonitrile

Table S20: QM-calculated values for the Gibbs free energy of activation for the O-alkylation ( $\Delta^\ddagger G_{\text{O}}^{\circ, \text{L}, \text{QM}}$ ) and the C-alkylation ( $\Delta^\ddagger G_{\text{C}}^{\circ, \text{L}, \text{QM}}$ ) pathways, the Gibbs free-energy difference ( $\Delta G_{\text{C-O}}^{\circ, \text{QM}}$ ), the selectivity ratio ( $k_{\text{O}}^{\text{QM}}/k_{\text{C}}^{\text{QM}}$ ) and the rate constants of the O-alkylation and C-alkylation pathways ( $k^{\text{QM}}$ ) of the reaction in acetonitrile at 298 K at all the levels of theory tested. The corresponding values obtained from the experiments fitted with Model 1+3 in this work are also reported for comparison. CI: Confidence Intervals

Level of theory	$\Delta^\ddagger G_{\text{O}}^{\circ, \text{L}, \text{QM}}$ /kJ mol <sup>-1</sup>	$\Delta^\ddagger G_{\text{C}}^{\circ, \text{L}, \text{QM}}$ /kJ mol <sup>-1</sup>	$\Delta G_{\text{C-O}}^{\circ, \text{QM}}$ /kJ mol <sup>-1</sup>	$k_{\text{O}}^{\text{QM}}/k_{\text{C}}^{\text{QM}}$	$k_{\text{O}}^{\text{QM}}$ /dm <sup>3</sup> mol <sup>-1</sup> s <sup>-1</sup>	$k_{\text{C}}^{\text{QM}}$ /dm <sup>3</sup> mol <sup>-1</sup> s <sup>-1</sup>
B3LYP/6-31G(d)	97.04	106.8	9.80	52.83	$1.750 \times 10^{-3}$	$3.313 \times 10^{-5}$
B3LYP/6-31+G(d)	93.25	102.5	9.27	43.03	$8.082 \times 10^{-3}$	$1.878 \times 10^{-4}$
B3LYP/6-311+G(d,p)	97.82	106.5	8.67	34.04	$1.241 \times 10^{-3}$	$3.646 \times 10^{-5}$
B3LYP/6-311++G(d,p)	98.02	106.5	8.51	31.77	$1.137 \times 10^{-3}$	$3.577 \times 10^{-5}$
B3LYP/6-311G(2d,d,p)	95.19	103.8	8.62	33.11	$3.575 \times 10^{-3}$	$1.080 \times 10^{-4}$
B3LYP/cc-pVDZ	103.0	113.5	10.46	68.97	$1.540 \times 10^{-4}$	$2.233 \times 10^{-6}$
B3LYP/cc-pVTZ	103.8	113.7	9.88	55.58	$1.128 \times 10^{-4}$	$2.029 \times 10^{-6}$
M05-2X/6-31G(d)	80.84	87.51	6.67	15.41	$1.350 \times 10^0$	$8.762 \times 10^{-2}$
M05-2X/6-31+G(d)	78.46	81.91	3.45	4.20	$3.571 \times 10^0$	$8.508 \times 10^{-1}$
M05-2X/6-31+G(d,p)	78.81	81.39	2.59	2.96	$3.096 \times 10^0$	$1.048 \times 10^0$
M05-2X/6-311++G(d,p)	87.07	88.65	1.57	1.97	$1.094 \times 10^{-1}$	$5.558 \times 10^{-2}$
M05-2X/cc-pVTZ	93.64	98.36	4.71	6.98	$7.641 \times 10^{-3}$	$1.095 \times 10^{-3}$
M06-2X/6-31+G(d)	87.06	88.99	1.93	2.24	$1.108 \times 10^{-1}$	$4.943 \times 10^{-2}$
M06-2X/6-311++G(d,p)	94.74	95.21	0.47	1.26	$5.000 \times 10^{-3}$	$3.952 \times 10^{-3}$
M06-2X/cc-pVDZ	98.04	101.7	3.68	4.56	$1.304 \times 10^{-3}$	$2.858 \times 10^{-4}$
M06-2X/cc-pVTZ	103.0	105.5	2.57	2.93	$1.790 \times 10^{-4}$	$6.105 \times 10^{-5}$
wB97xD/6-31+G(d)	83.39	85.50	2.11	2.33	$4.785 \times 10^{-1}$	$2.052 \times 10^{-1}$
wB97xD/6-311++G(d,p)	91.77	91.70	-0.06	1.01	$1.594 \times 10^{-2}$	$1.584 \times 10^{-2}$
			$\Delta G_{\text{C-O}}^{\circ}$ /kJ mol <sup>-1</sup>	$k_{\text{O}}/k_{\text{C}}$	$k_{\text{O}}$ /dm <sup>3</sup> mol <sup>-1</sup> s <sup>-1</sup>	$k_{\text{C}}$ /dm <sup>3</sup> mol <sup>-1</sup> s <sup>-1</sup>
Expt.			7.31	18.72	$1.809 \times 10^{-2}$	$9.659 \times 10^{-4}$
95% CI					$[0.000-4.642] \times 10^{-2}$	$[0.000-27.38] \times 10^{-4}$

## QM-calculated values in methanol

Table S21: QM-calculated values for the Gibbs free-energy of activation for the O-alkylation ( $\Delta^\ddagger G_{\text{O}}^{\text{o,L,QM}}$ ) and the C-alkylation ( $\Delta^\ddagger G_{\text{C}}^{\text{o,L,QM}}$ ) pathways, the Gibbs free-energy difference ( $\Delta G_{\text{C-O}}^{\text{o,QM}}$ ), the selectivity ratio ( $k_{\text{O}}^{\text{QM}}/k_{\text{C}}^{\text{QM}}$ ) and the rate constants of the O-alkylation and C-alkylation pathways ( $k^{\text{QM}}$ ) of the reaction in methanol at 298 K at all the levels of theory tested. The corresponding values obtained from the experiments fitted with Model 1+2+3+4 in this work are also reported for comparison. CI: Confidence Intervals

Level of theory	$\Delta^\ddagger G_{\text{O}}^{\text{o,L,QM}}$ /kJ mol <sup>-1</sup>	$\Delta^\ddagger G_{\text{C}}^{\text{o,L,QM}}$ /kJ mol <sup>-1</sup>	$\Delta G_{\text{C-O}}^{\text{o,QM}}$ /kJ mol <sup>-1</sup>	$k_{\text{O}}^{\text{QM}}/k_{\text{C}}^{\text{QM}}$	$k_{\text{O}}^{\text{QM}}$ /dm <sup>3</sup> mol <sup>-1</sup> s <sup>-1</sup>	$k_{\text{C}}^{\text{QM}}$ /dm <sup>3</sup> mol <sup>-1</sup> s <sup>-1</sup>
B3LYP/6-31G(d)	102.2	107.9	5.67	10.00	$2.173 \times 10^{-4}$	$2.174 \times 10^{-5}$
B3LYP/6-31+G(d)	99.13	103.7	4.57	6.42	$7.529 \times 10^{-4}$	$1.172 \times 10^{-4}$
B3LYP/6-311+G(d,p)	102.8	107.0	4.27	5.75	$1.687 \times 10^{-4}$	$2.932 \times 10^{-5}$
B3LYP/6-311++G(d,p)	103.1	107.1	4.03	5.23	$1.499 \times 10^{-4}$	$2.866 \times 10^{-5}$
B3LYP/6-311G(2d,d,p)	99.34	104.2	4.83	7.19	$6.763 \times 10^{-4}$	$9.402 \times 10^{-5}$
B3LYP/cc-pVDZ	107.9	115.1	7.14	18.06	$2.144 \times 10^{-5}$	$1.187 \times 10^{-6}$
B3LYP/cc-pVTZ	108.5	114.6	6.05	11.83	$1.679 \times 10^{-5}$	$1.419 \times 10^{-6}$
M05-2X/6-31G(d)	86.67	88.59	1.93	2.27	$1.292 \times 10^{-1}$	$5.691 \times 10^{-2}$
M05-2X/6-31+G(d)	84.20	82.44	-1.76	0.51	$2.866 \times 10^{-1}$	$5.602 \times 10^{-1}$
M05-2X/6-31+G(d,p)	85.28	82.37	-2.91	0.31	$2.289 \times 10^{-1}$	$7.103 \times 10^{-1}$
M05-2X/6-311++G(d,p)	92.87	88.95	-3.93	0.20	$1.062 \times 10^{-2}$	$4.950 \times 10^{-2}$
M05-2X/cc-pVTZ	99.52	99.04	-0.48	0.85	$7.165 \times 10^{-4}$	$8.336 \times 10^{-4}$
M06-2X/6-31+G(d)	93.71	90.68	-3.03	0.30	$7.617 \times 10^{-3}$	$2.520 \times 10^{-2}$
M06-2X/6-311++G(d,p)	100.4	95.79	-4.59	0.16	$5.815 \times 10^{-4}$	$3.152 \times 10^{-3}$
M06-2X/cc-pVDZ	102.7	102.5	-0.21	0.95	$2.003 \times 10^{-4}$	$2.108 \times 10^{-4}$
M06-2X/cc-pVTZ	108.2	106.4	-1.72	0.52	$2.208 \times 10^{-5}$	$4.266 \times 10^{-5}$
wB97xD/6-31+G(d)	91.08	87.58	-3.50	0.24	$2.168 \times 10^{-2}$	$8.904 \times 10^{-2}$
wB97xD/6-311++G(d,p)	97.73	93.45	-4.28	0.18	$1.433 \times 10^{-3}$	$7.879 \times 10^{-3}$
			$\Delta G_{\text{C-O}}^{\text{o}}$ /kJ mol <sup>-1</sup>	$k_{\text{O}}/k_{\text{C}}$	$k_{\text{O}}$ /dm <sup>3</sup> mol <sup>-1</sup> s <sup>-1</sup>	$k_{\text{C}}$ /dm <sup>3</sup> mol <sup>-1</sup> s <sup>-1</sup>
Expt.			2.89	2.81	$7.584 \times 10^{-4}$	$2.703 \times 10^{-4}$
95% CI					$[0.00-18.34] \times 10^{-4}$	$[0.000-7.202] \times 10^{-4}$

Table S22: QM-calculated free energy of solvation ( $\Delta G_{\text{O}}^{\text{o,solv}}$ ) at 298 K and free-energy differences ( $G^{\text{o,L}} - G^{\text{o,IG}}$ ) between acetonitrile and methanol for sodium  $\beta$ -naphthoxide, benzyl bromide and transition state structures for the O-alkylation pathway ( $\text{TS}_{\text{O}_2}$ ) and the C-alkylation pathway ( $\text{TS}_{\text{C}}$ ) in 4 levels of theory. The differences of these values in acetonitrile and methanol are also reported.

Level of theory	Species	$\Delta G^{\text{o,solv}}/\text{kJ mol}^{-1}$		$\Delta\Delta G^{\text{o,solv}}/\text{kJ mol}^{-1}$	$G^{\text{o,L}} - G^{\text{o,IG}}/\text{kJ mol}^{-1}$		$G_{\text{acet}}^{\text{o,L}} - G_{\text{meth}}^{\text{o,L}}/\text{kJ mol}^{-1}$
		Acetonitrile	Methanol		Acetonitrile	Methanol	
B3LYP/6-31G(d)	Sodium $\beta$ -naphthoxide	-101.23	-104.83	3.61	-103.46	-103.32	-0.14
	Benzyl bromide	-34.73	-31.17	-3.56	-31.17	-27.54	-3.63
	$\text{TS}_{\text{O}_2}$	-125.07	-119.93	-5.13	-127.66	-121.81	-5.85
	$\text{TS}_{\text{C}}$	-116.21	-115.20	-1.01	-120.58	-118.40	-2.17
M05-2X/6-31G(d)	Sodium $\beta$ -naphthoxide	-110.31	-115.28	4.97	-112.23	-113.71	1.48
	Benzyl bromide	-38.20	-34.64	-3.56	-38.09	-34.56	-3.53
	$\text{TS}_{\text{O}_2}$	-129.10	-124.69	-4.41	-132.70	-126.36	-6.34
	$\text{TS}_{\text{C}}$	-122.30	-122.63	0.33	-124.44	-124.51	0.08
M05-2X/6-31+G(d,p)	Sodium $\beta$ -naphthoxide	-113.09	-118.75	5.66	-115.78	-121.27	5.49
	Benzyl bromide	-41.20	-37.64	-3.56	-40.61	-36.84	-3.77
	$\text{TS}_{\text{O}_2}$	-135.40	-131.04	-4.37	-141.32	-135.80	-5.51
	$\text{TS}_{\text{C}}$	-131.85	-132.98	1.12	-134.79	-135.96	1.17
M05-2X/cc-pVTZ	Sodium $\beta$ -naphthoxide	-112.23	-117.06	4.83	-113.63	-117.49	3.85
	Benzyl bromide	-38.71	-35.17	-3.54	-37.43	-33.81	-3.62
	$\text{TS}_{\text{O}_2}$	-134.32	-129.71	-4.60	-136.18	-133.19	-2.99
	$\text{TS}_{\text{C}}$	-129.47	-130.06	0.59	-132.31	-133.34	1.02

## Wigner tunnelling correction factor

The Wigner tunnelling factor<sup>1</sup> is given as

$$\kappa = 1 + \frac{1}{24} \left( \frac{h\nu^\ddagger}{k_{\text{B}}T} \right)^2, \quad (\text{S-1})$$

where  $\nu^\ddagger$  is the value of the imaginary frequency of the transition state structure in  $\text{cm}^{-1}$ .

## References

- (1) E. Wigner, Calculation of the Rate of Elementary Association Reactions, *J. Chem. Phys.*, 1937, **5**, 720–725.
- (2) T. Kimura, T. Matsushita, K. Ueda, K. Tamura, S. Takagi, Deuterium Isotope Effect on Excess Enthalpies of Methanol or Ethanol and Their Deuterium Derivatives at 298.15 K, *J. Therm. Anal. Calorim.*, 2001, **64**, 231–241.
- (3) Process Systems Enterprise, gPROMS, [www.psenterprise.com/gproms](http://www.psenterprise.com/gproms), 1997-2018